

Tuning the chemical hardness of boron nitride nanosheets by doping carbon for enhanced adsorption capacity

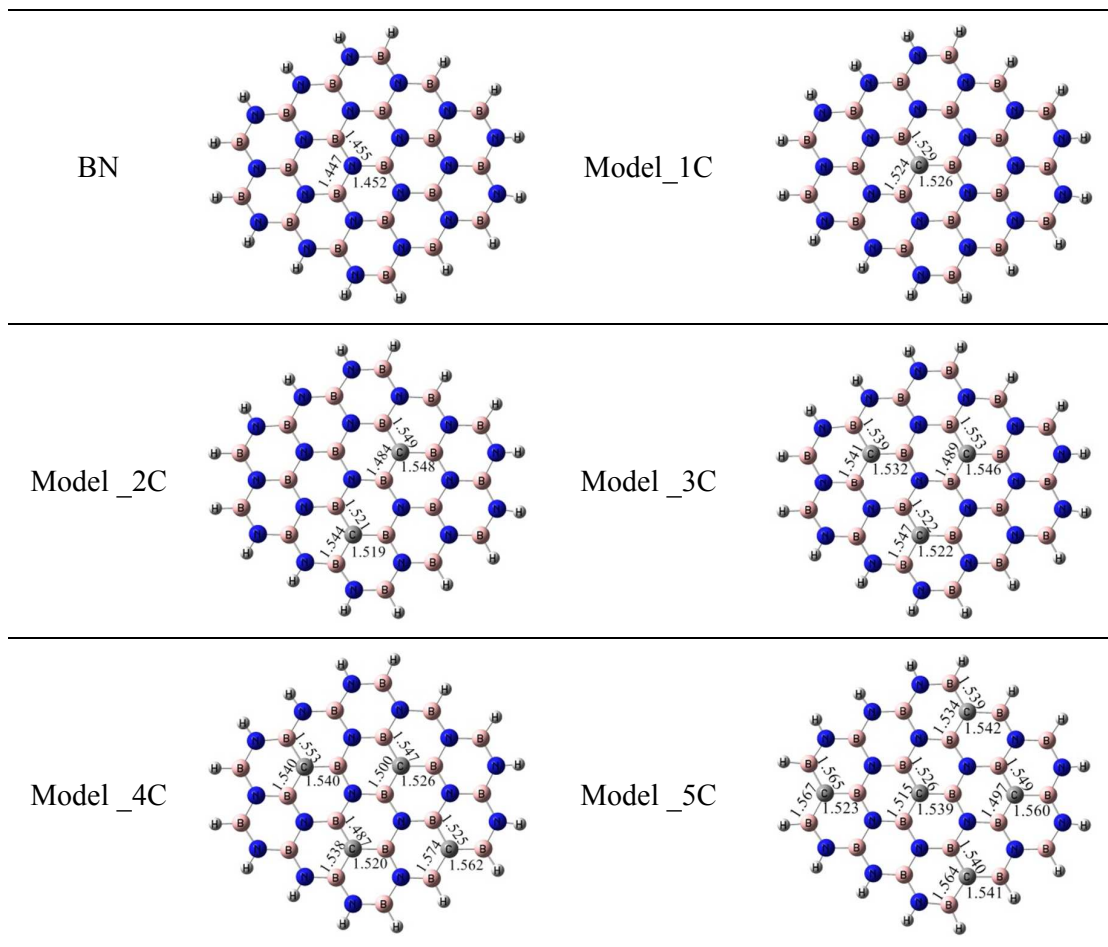
Hongping Li,^a Siwen Zhu,^b Ming Zhang,^a Peiwen Wu,^b Jingyu Pang,^b Wenshuai

Zhu,^{*b} Wei Jiang,^a and Huaming Li^{*a}

^a *Institute for Energy Research, Jiangsu University, Zhenjiang 212013, P. R. China*

^b *School of Chemistry and Chemical Engineering, Jiangsu University, Zhenjiang
212013, P. R. China*

Figure S1. The stable configurations of BN, Model_xC (x=1, 2, 3, 4, 5) and some important bond lengths (unit: Å).



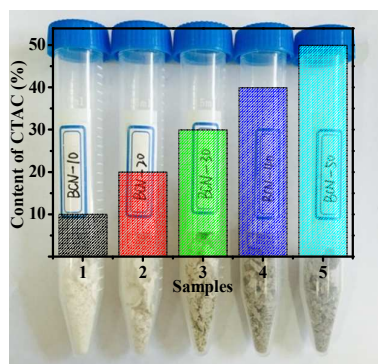


Figure S2. Colors for different BCN-*x* samples.

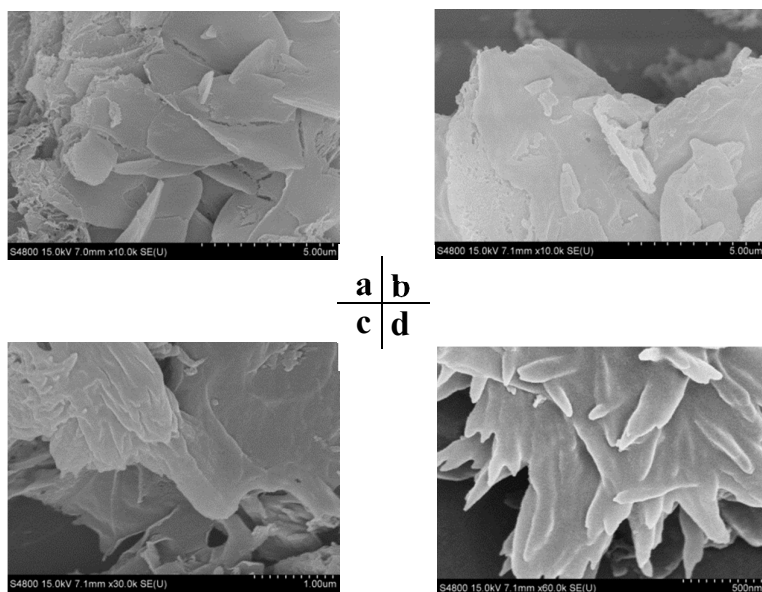


Figure S3. SEM of BCN-10 (a); BCN-20 (b); BCN-30 (c); BCN-50 (d).

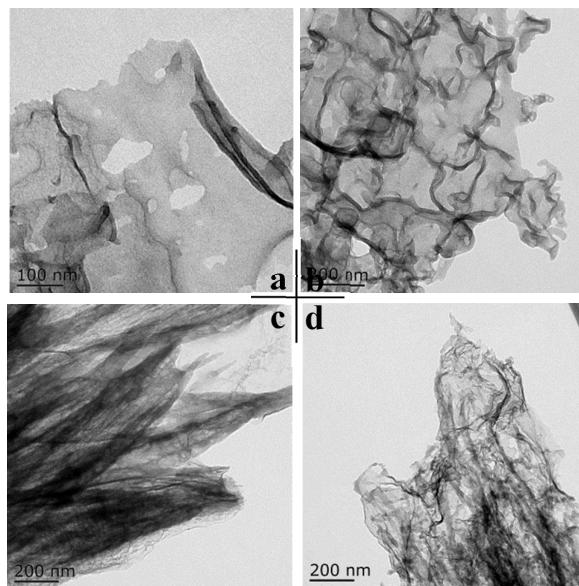


Figure S4. TEM of BN-10 (a); BCN-20 (b); BCN-30 (c); BCN-50 (d);

Table S1. Atomic concentrations of B, C, N, O in BN and BCN-x.

	B	N	C	O
BN	39.14	38.47	12.36	10.03
BCN-10	38.66	36.73	13.72	10.89
BCN-20	36.53	32.68	17.79	12.99
BCN-30	37.7	34.05	14.04	14.21
BCN-40	35.26	31.76	18.89	14.1
BCN-50	33.13	29.53	23.26	14.08

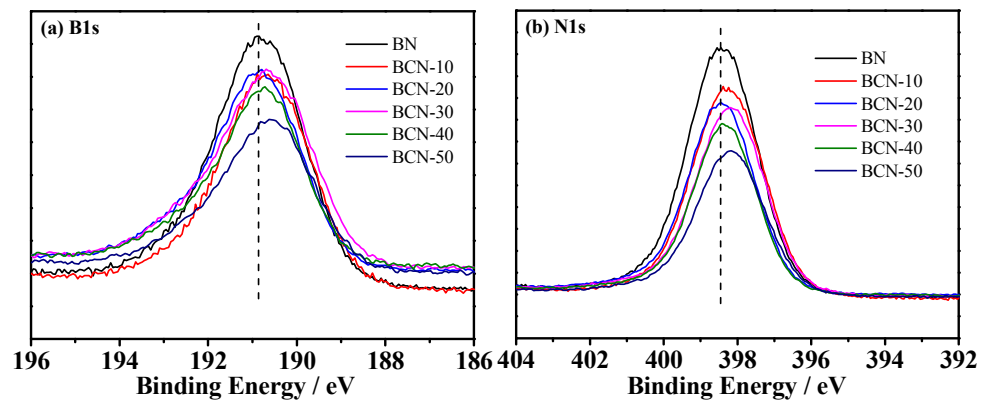


Figure S5. XPS spectra of BN and BCN-x, (a) B 1s, (b) N 1s.

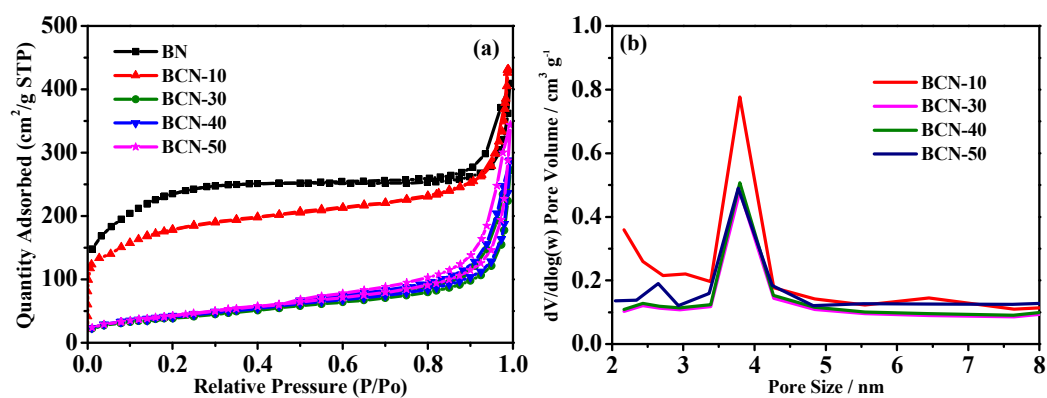


Figure S6. (a) N_2 adsorption-desorption isotherms of different adsorbents and (b)

Barrett-Joyner-Halenda (BJH) pore size distribution curve of BN, BCN- x .

Table S2. Textual properties of different samples.

Sample	S_{BET} ($\text{m}^2 \text{g}^{-1}$)	Pore Size (nm)
BN	772.3	55.6
BCN-10	608.5	6.8
BCN-30	146.8	12.6
BCN-40	155.1	12.6
BCN-50	160.4	11.1

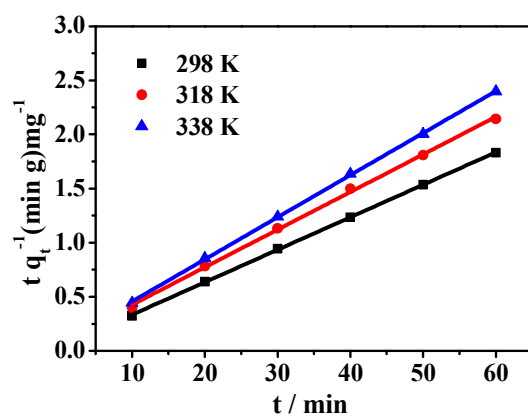


Figure S7. The plots of pseudo-second-order kinetic model for DBT adsorption on the BCN-50 at different temperature.

Table S3. Pseudo-second-ordered kinetic parameters for adsorption DBT on BCN-50

at different temperature

Parameters	298 K	318 K	338 K
q_e (mg g ⁻¹)	33.28	28.77	25.72
K_2 (mg g ⁻¹ min ⁻¹)	27.65×10 ⁻³	15.64×10 ⁻³	22.16×10 ⁻³
h (mg g ⁻¹ min ⁻¹)	30.63	12.95	14.66
R^2	0.9998	0.9986	0.9998

To investigate the adsorption kinetics, the kinetic order, adsorption rate and adsorption rate constant for the adsorption DBT on h-BCN materials were studied. The pseudo-first-order model (eq. X) and pseudo-second-order model (eq. X) were presented as follows:

$$\lg(q_e - q_t) = \lg q_e - k_1 t \quad (1)$$

$$\frac{t}{q_t} = \frac{1}{k_2 q_e^2} + \frac{t}{q_e} \quad (2)$$

The initial adsorption rate h (mg g⁻¹ min⁻¹) was given by the following equation:

$$h = k_2 q_e^2 \quad (3)$$

where q_e is the amount of DBT adsorbed at equilibrium (mg g⁻¹), q_t is the amount of DBT adsorbed at time t (mg g⁻¹), k_1 is the pseudo-first-order rate constant (min⁻¹), and k_2 is the pseudo-second-order rate constant (g mg⁻¹ min⁻¹). As shown in Figure S7, the adsorption of DBT on BCN-50 fits well to the pseudo-second-order model, the correlation coefficient values for which are all above 0.99.

Table S4. Adsorptive energies for DBT by different (Model_xC, x=1~5) model

materials.

Model systems	Adsorptive energy (kcal/mol)
h-BN_DBT	-20.12
Model _C _DBT	-20.16
Model _2C _DBT	-22.63
Model _3C _DBT	-37.73
Model _4C _DBT	-24.19
Model _5C _DBT	-75.70